Ephrin-B2 Reverse Signaling Increases α5β1 Integrin–Mediated Fibronectin Deposition and Reduces Distal Lung Compliance

Katherine M. Bennett[1]*, Maria D. Afanador[1]*, Charitharth V. Lal[1], Haiming Xu[1], Elizabeth Persad[1], Susan K. Legan[1], George Chenaux[2], Michael Dellinger[3], Rashmin C. Savani[1], Christopher Dravis[2], Mark Henkemeyer[2], and Margaret A. Schwarz[1]

[1]Department of Pediatrics, [2]Department of Developmental Biology, and [3]Department of Surgery, University of Texas Southwestern Medical Center at Dallas, Dallas, Texas

Alveolar growth abnormalities and severe respiratory dysfunction are often fatal. Identifying mechanisms that control epithelial proliferation and enlarged, poorly septated airspaces is essential in developing new therapies for lung disease. The membrane-bound ligand ephrin-B2 is strongly expressed in lung epithelium, and yet in contrast to its known requirement for arteriogenesis, considerably less is known regarding the function of this protein in the epithelium. We hypothesize that the vascular mediator ephrin-B2 governs alveolar growth and mechanics beyond the confines of the endothelium. We used the *in vivo* manipulation of ephrin-B2 reverse signaling to determine the role of this vascular mediator in the pulmonary epithelium and distal lung mechanics. We determined that the ephrin-B2 gene (*EfnB2*) is strongly expressed in alveolar Type 2 cells throughout development and into adulthood. The role of ephrin-B2 reverse signaling in the lung was assessed in *Efnb2*$^{LacZ/6YF\Delta V}$ mutants that coexpress the intracellular truncated ephrin-B2–β-galactosidase fusion and an intracellular point mutant ephrin-B2 protein that is unable to become tyrosine-phosphorylated or to interact with either the SH2 or PDZ domain–containing downstream signaling proteins. In these viable mice, we observed pulmonary hypoplasia and altered pulmonary mechanics, as evidenced by a marked reduction in lung compliance. Associated with the reduction in lung compliance was a significant increase in insoluble fibronectin (FN) basement membrane matrix assembly with FN deposition, and a corresponding increase in the α5 integrin receptor required for FN fibrillogenesis. These experiments indicate that ephrin-B2 reverse signaling mediates distal alveolar formation, fibrillogenesis, and pulmonary compliance.

CLINICAL RELEVANCE

The vascular mediator ephrin-B2 is widely expressed in pulmonary alveolar Type II epithelial cells during lung development, and in the adult lung, reverse ephrin-B2 signaling mediates alveolar morphometry and distal lung mechanics. The disruption of ephrin-B2 in distal lung mechanics is associated with alterations in distal alveolar extracellular matrix deposition. These findings are relevant to a better understanding of those factors that control pulmonary mechanics, and may have therapeutic potential.

Keywords: arterial; fibronectin; α5β1 integrin; alveoli; pulmonary mechanics

Lung development in mammalian species occurs through a series of overlapping stages, distinguished in terms of their histological appearance, and specifically the growth and differentiation of pulmonary epithelial structures. Although the proximal airways are completely formed by the end of gestation, the distal airways and alveoli continue their growth and maturation beyond the time of birth. Concurrent to the development of the epithelial structures, the pulmonary vasculature develops in a sequential fashion, via the coordinated processes of angiogenesis and vasculogenesis (1). Because of the close proximity of the developing airways and vasculature in the lung, vascular mediators have been suggested to influence pulmonary development. For instance, Chen and colleagues (2) and Schwarz and colleagues (3–5) used a mouse fetal lung allograft model to show that endothelial–monocyte activating polypeptide II can not only inhibit neovascularization, but can also significantly impair epithelial morphogenesis. Based on these and similar findings, our laboratory has focused on the role of vascular mediators during pulmonary development.

Our studies have focused on the ephrin-B2 (EfnB2) ligand expressed on primitive arterial vessels, and have distinguished the arterial domains during murine development. Ephrins and their Eph receptors are transmembrane-bound proteins that function as a receptor–ligand pair in transmitting signals in a bidirectional fashion via cell-to-cell contact–mediated interactions (6). As a member of the receptor tyrosine kinase family, the Eph receptor undergoes autophosphorylation upon binding to its ephrin ligand, activating a downstream signaling cascade via a process known as forward signaling. Moreover, ephrins can activate signal transduction pathways themselves after interactions with the Eph receptor, upon the tyrosine phosphorylation of their cytoplasmic tail in the process known as reverse signaling. This bidirectional signaling is thought to communicate signals that regulate the cytoskeleton during axon pathfinding, cell

(*Received in original form January 2, 2013 and in final form May 21, 2013*)

* These authors contributed equally to this work.

This work was supported by National Institutes of Health grants HL60061 (M.A.S.), HL75764 (M.A.S.), HL114977 (M.A.S.), MH066332 (M.H.), HL079090 (R.C.S.), HL075930 (R.C.S.), and HL093535 (R.C.S.), by a Klaus Pediatric Research Award (K.M.B.), by the Children's Clinical Research Advisory Committee (M.A.S. and R.C.S.), and by the University of Texas Southwestern Simmons Comprehensive Cancer Center (M.A.S.).

Author Contributions: K.M.B., M.D.A., C.V.L, H.X., E.P., S.K.L., G.C., M.D., R.C.S., and C.D. were responsible for the acquisition of data or the analysis and interpretation of data. M.H. and M.A.S. were responsible for the conception and design of this study, and were also responsible for drafting the manuscript for important intellectual content.

Correspondence and requests for reprints should be addressed to Margaret A. Schwarz, M.D., Department of Pediatrics, University of Texas Southwestern Medical Center at Dallas, 5323 Harry Hines Boulevard, K4.220, Dallas, TX 75390. E-mail: margaret.schwarz@utsouthwestern.edu

This article has an online supplement, which is accessible from this issue's table of contents at www.atsjournals.org

Am J Respir Cell Mol Biol Vol 49, Iss. 4, pp 680–687, Oct 2013

Originally Published in Press as DOI: 10.1165/rcmb.2013-0002OC on June 6, 2013
Internet address: www.atsjournals.org

migration, cell adhesion, and vascular remodeling. Ephrins can be divided into two subclasses, A and B, based on their structural features and binding affinities (7, 8). The focus of our work is on the B subclass ephrin, EfnB2. Its structure consists of an extracellular receptor–binding domain and an intracellular cytoplasmic tail composed of six tyrosine residues that become phosphorylated and bind SH2 domain proteins such as Grb4, and a terminal valine residue that binds PDZ domain proteins such as Pick1.

EfnB2 is expressed predominantly by arterial endothelial cells, whereas one of its cognate receptors, EphB4, is predominantly found on the venous endothelium (9). However, targeted disruption of the Efnb2 gene affects both venous and arterial remodeling, suggesting that reciprocal interactions are necessary for angiogenesis (10). In addition, EfnB2 is necessary for the formation of embryonic vasculature, because mice lacking EfnB2 die *in utero* before embryonic Day 11.5 from defects in vascular remodeling (9). EfnB2 plays a role in various morphogenetic processes, including axon guidance and pathfinding (11), smooth muscle cell spreading, motility, and adhesion during blood-vessel wall assembly (12), the maturation of cardiac valve leaflets (8), lymphatic remodeling (13), and cloacal septation and urorectal development (14), among others. Although EfnB2 has been shown to play a role in arterial morphogenesis, little is known about the role of EfnB2 in lung development. It is known that EfnB2 expression is not limited to arterial endothelial cells during lung development (15), because mice homozygous for the hypomorphic knock-in allele encoding a mutant EfnB2 cytoplasmic domain exhibit abnormal elastic matrix formation and postnatal distal alveolar defects (16), and EfnB2 plays a role in distal alveolar repair after hyperoxia (17). However, the cellular distribution of EfnB2 and its impact on extracellular matrix formation and pulmonary mechanics remain unknown.

Here we show for the first time a role for EfnB2 reverse signaling in pulmonary development. We demonstrate that EfnB2 is widely expressed in pulmonary alveolar Type II epithelial cells throughout lung development and in the adult lung. Furthermore, EfnB2 reverse signaling regulates distal alveolar crest and airway formation, because alterations in signaling not only reduced crest formation significantly, but also induced alveolar dysplasia. In conjunction with the alterations in distal airway morphometry, a marked disruption in distal lung mechanics was evident, with a reduction in lung compliance that was directly associated with a marked increase in distal lung fibronectin (FN) fibrillogenesis and matrix deposition. These experiments indicate that EfbnB2 reverse signaling is necessary for distal alveolar formation, for limiting fibrillogenesis, and for normal pulmonary compliance.

MATERIALS AND METHODS

Animals

EfnB2$^{\mathrm{LacZ/6YF\Delta V}}$ mutants were generated by combining the LacZ and 6YFΔV alleles, as previously described (18). In brief, the *EfnB2*$^{\mathrm{LacZ}}$ mutation replaces the protein's cytoplasmic tail with an in-frame *LacZ* cassette, resulting in the expression of an ephrin-B2–β-galactosidase (β-gal) fusion protein (14) (19), and the *EfnB2*$^{\mathrm{6YF\Delta V}}$ allele deletes the C-terminal valine residue and replaces the six tyrosine residues with phenylalanine (18). *EfnB2*$^{\mathrm{LacZ/6YF\Delta V}}$ mutants and wild-type (WT) littermates were maintained in a mixed 129/CD1 strain background. All animal procedures were approved by our Institutional Animal Care and Use Committee, in accordance with National Institutes of Health guidelines.

Protein Isolation and Western Blotting

Protein for Western blotting analysis was obtained from distal lung tissue, snap-frozen, and pulverized, and the powder was suspended in radio immunoprecipitation buffer lysis buffer (i.e., 150 mM NaCl, 50 mM Tris, pH 8.0, 1% NP-40, 0.25% deoxycholate (DOC), and 0.1% SDS) with 5 μl of protease inhibitor. Samples were homogenized using an ultrasonic processor (Cole-Parmer, Court Vernon Hills, IL). After protein quantification (Bio-Rad, Hercules, CA), equal protein amounts of samples were electrophoresed, transferred using a semidry transfer, and blocked in milk in Tris-buffered saline and Tween 20 (i.e., 5 M NaCl, 1 M Tris-HCl, pH 7.4, and 0.05% Tween-20). They were then incubated in the primary antibody solution, rinsed, exposed to secondary antibodies, and revealed using Amersham ECL Western Blotting Detection Reagents (catalogue number RPN 2106; GE Healthcare, Knox, IN). Primary antibodies included rabbit anti-Aquaporin 5 (AQP5) (catalog number AB 15858; Millipore, Billerica, MA), mouse anti-actin (catalogue number MAB 1501; Millipore), FN (Abcam, Cambridge, MA), and α5 integrin (Chemicon, Billerica, MA). Specific binding was detected using a chemiluminescence substrate (Pierce, Rockford, IL) and XAR-5 film (Eastman Kodak, Rochester, NY). Quantitative analysis was performed using Quantity One Software (Bio-Rad), and samples were normalized against actin.

Insoluble and Soluble FN Analysis

Some of the pulverized distal lung powder was suspended in a DOC lysis buffer (2% sodium deoxycholate, 0.02 M Tris-HCl, pH 8.8, 2 mM PMSF, 2 mM EDTA, 2 mM iodoacetic acid, and 2 mM *N*-ethylmaleimide), passed through a 26-gauge needle, and centrifuged at 15 × *g* for 20 minutes at 4°C. The supernatant containing the DOC-soluble component was collected, and the DOC-insoluble pellet was solubilized using SDS lysis buffer (1% SDS, 25 mM Tris-HCl, pH 8.0, 2 mM PMSF, 2 mM EDTA, 2 mM iodoacetic acid, and 2 mM *N*-ethylmaleimide). Reduced lysates were separated on SDS-PAGE gels and probed with an anti-FN antibody (catalog number sc-9068; Santa Cruz Biotechnology, Santa Cruz, CA). Under reducing conditions, high-molecular-weight FN multimers resolve as a 220-kD band. Semiquantitative densitometry was performed as previously described (20).

Inflation Fixation and Tissue Harvest

Mice were sedated and killed according to Institutional Animal Care and Use Committee guidelines. The abdomen was entered and the aorta was cut to allow blood to drain from the lungs. Keeping the chest wall intact, the trachea was exposed and cannulated with a 20-gauge angiocatheter, and inflated with 4% paraformaldehyde at 25 cm Hg pressure. The inflation-fixed lungs and hearts were excised *en bloc*, fixed in 4% PFA, and embedded in paraffin, and processed into 5-μm sections for histological analysis.

Immunohistochemistry

Five-micron sections were deparaffinized and rehydrated, endogenous peroxidase activity was quenched and blocked, and the sections were incubated with primary antibodies overnight at 4°C. Sections were then rinsed and incubated with secondary antibody, and the primary antibodies (catalog number SPC AB 3786; Chemicon), FN (catalog number ab23750; Abcam), α–smooth muscle actin (catalog number A5228; Sigma Chemical Company, St. Louis, MO), AQP5 (catalog number AB15858; Millipore), LYVE-1 (catalog number ab14917; Abcam), Ki67 (catalog number ab15580; Abcam), and pro–surfactant protein C (pro-SPC, catalog number 07-647; Millipore) were revealed with either AEC chromogen solution or conjugated fluorescence secondary antibodies Alexa Fluor 488 (Invitrogen, Carlsbad, CA) or Cy3-conjugated goat anti-rabbit IgG (Jackson Immuno Research Laboratory, West Grove, PA). Coverslips were mounted onto the slides, using Slow Fade Gold Anti-Fade reagent with 4′6-diamidino-2-phenylindole (catalog number S36938; Invitrogen). Some slides underwent hematoxylin-and-eosin and trichrome staining.

X-Gal Staining

Tissue samples were embedded in optimal cutting temperature (OCT), cryosectioned, air-dried at room temperature, and then immersed in LacZ fix buffer (0.2% glutaraldehyde, 5 mM EGTA, 2 mM $MgCl_2$, and PBS) at room temperature, rinsed several times in

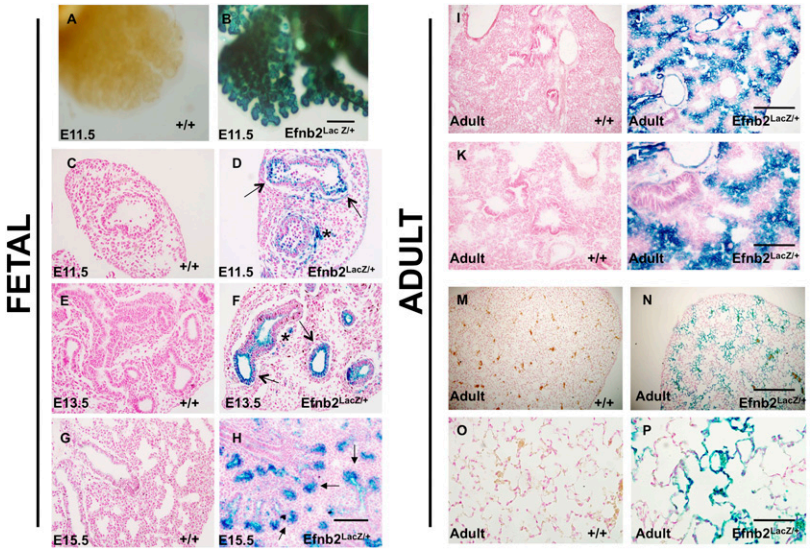

Figure 1. Ephrin-B2 (EfnB2) is strongly expressed in the distal alveolar region throughout development and during adulthood. Fetal lungs were isolated from timed pregnant wild-type (WT; +/+) and Efnb2$^{LacZ/+}$ transgenic mice. The analysis of sections from different time points in lung development indicated that Efnb2 is expressed throughout lung development in distal epithelial regions on embryological (E) Day 11.5 in whole-mount (*B*) and paraffin-embedded (*D*) sections, and was maintained throughout development, as seen on representative Days E13.5 and E15.5 (*F* and *H*; *arrows* denote epithelial regions, and *asterisks* denote vascular regions), in contrast to littermate WT control mice (*A*, *C*, *E*, and *G*). The distal alveolar expression of EfnB2 was maintained into adulthood (8 wk), when distal lung tissue demonstrated striking regional Efnb2–LacZ expression in collapsed (*J* and *L*) and inflation-fixed (*N* and *P*) lungs, compared with WT (*I*, *K*, *M*, and *O*) littermates. Magnification, *A* and *B*, *scale bar* = 250 μm; *C–H*, *scale bar* = 50 μm; *I*, *J*, *M*, and *N*, *scale bar* = 100 μm.

wash buffer (2 mM $MgCl_2$, 0.02% NP-40, and PBS), and incubated at 37°C overnight in LacZ staining buffer. The slides were then rinsed, fixed, and counterstained with nuclear fast red before being assessed via light microscopy. For the whole-mount staining of embryonic lungs, tissues were cleared in benzyl alcohol/benzyl benzoate, and images were recorded using a NeoLumar dissecting microscope (Zeiss, Cambridge, UK) and a DP-70 camera (Olympus, Center Valley, PA). Some lungs were transiently inflation-fixed at 25 mm Hg for 15 minutes in 4% PFA, before proceeding with tissue-processing in OCT and LacZ staining.

Nuclear Fast Red Staining

Tissue sections from paraffin-embedded lungs were deparaffinized in xylenes and rehydrated in decreasing concentrations of ethanol, washed in PBS, immersed in nuclear fast red stain for 30 seconds, and mounted.

Morphologic Analysis

Quantitative morphologic analyses were determined via the mean linear intercept (MLI) measurement using ImageJ software, provided by the National Institutes of Health (Bethesda, MD). After blinding of the data, MLIs were determined in four representative alveolar regions at ×600 magnification from each animal, and averaged for comparisons (21). Graphical analyses of randomized digital images from distal airways were used for secondary crest analyses. Three images per animal were quantified as previously described (16).

Ratios of Wet to Dry Weights of Lungs

Before dissection, anesthetized animals were weighed for total body weight. The left lung of each animal was dissected and weighed. The lungs were placed at 90°C for 48 hours, and then reweighed.

Ratios of Heart Weight to Body Weight

Anesthetized mice were weighed, and the weights of their hearts were obtained after dissection. Ratios of heart weight to total body weight were determined.

Pulmonary Function Tests

Lung function analysis. Forced oscillatory measurements to determine respiratory system impedance (Z_{rs}) and quasistatic transrespiratory pressure–volume ($P_{st,rs}$–V) data were obtained using a flexiVent rodent ventilator (SCIREQ, Quebec City, PQ, Canada). Anesthesia was induced by the intraperitoneal injection of a ketamine cocktail (100 mg/kg ketamine and 10 mg/kg xylazine). Once the mice were anesthetized, their tracheas were cannulated using an 18-gauge blunt-tipped catheter. The mice were then connected to the ventilator and ventilated at a rate of 150 breaths/minute, a tidal volume of 10 ml/kg, a positive end-expiratory pressure of 3 cm H_2O, and a fraction of inspired oxygen at 100% ($F_{I_{O_2}}$). Before the initiation of measurements, atropine was delivered, followed by the induction of muscle paralysis by an intraperitoneal injection of 0.5 mg/kg succinylcholine (Sigma Chemical

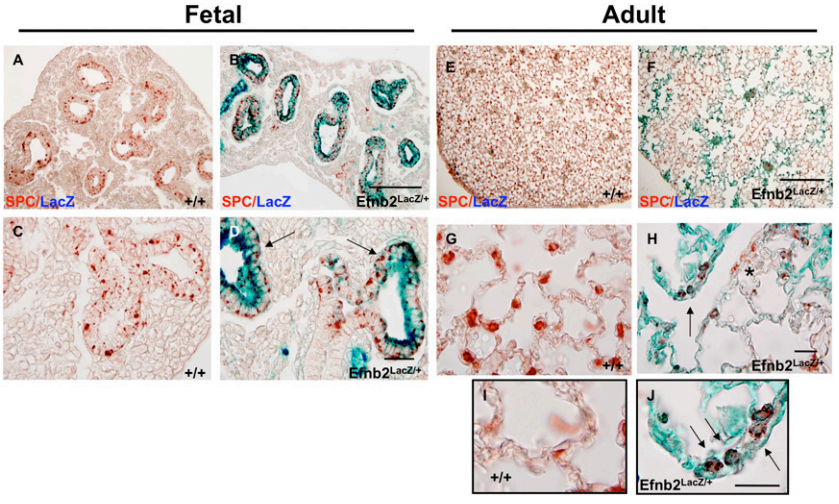

Figure 2. Alveolar Type II cell surfactant protein C (SPC) colocalizes with EfnB2 in the fetal and adult lung. Colocalization of β-galactosidase (β-gal) with the Type II alveolar cell marker surfactant protein C (immunohistochemistry, *red* AEC staining) in EfnB2$^{LacZ/+}$ mice confirms fetal epithelial cell Efnb2 expression (*B* and *D*, *arrows* indicate SPC/β-gal–positive cells), which was maintained into adulthood in some regions (*F*, *H*, and *J*, *arrows*, but not all SPC-positive cells are β-gal–positive, because SPC-positive cells occur with β-gal staining, as indicated by the *asterisk* in *H*), compared with littermate WT control mice (*A*, *C*, *E*, *G*, and *I*). Magnification in *A* and *B*, *scale bar* = 50 μm; in *C* and *D*, *scale bar* = 20 μm; in *E* and *F*, *scale bar* = 50 μm; in *G* and *H*, *scale bar* = 20 μm; and in *I* and *J*, *scale bar* = 20 μm.

Company). Throughout the experiment, mice were monitored using a continuous, nonrecording three-lead electrocardiogram.

Forced oscillatory measurements. A low-frequency oscillatory technique was performed, and the Z_{rs} was fitted to the constant-phase model that allows for the partitioning of airway and parenchymal tissue resistance. Results are reported as central airway resistance, tissue damping, tissue elastance, and tissue hysteresivity. Briefly, after volume-history standardization (three consecutive deep inflation/total lung capacity maneuvers), mice were ventilated for 5 minutes, and four consecutive prime eight maneuvers were executed. Data from all maneuvers were merged, and are represented as means ± SEMs.

Quasistatic P–V curves. After the completion of impedance measurements, the volume history was reset as already described, the subject was ventilated for an additional 5 minutes at 100% FiO_2 and then disconnected from the ventilator, and the tracheal canula was occluded for 5 minutes to allow the lungs to degas and achieve residual volume. At the conclusion of this step, the mouse was reconnected to the ventilator at zero positive end-expiratory pressure, and four consecutive pressure–volume loops were performed with stepwise inflation to 40 ml/kg. Data are represented both as the plotted, mean pressure–volume relationship and the P–V hysteresis, and we calculated the specific static respiratory system compliance for each experimental group.

Statistical Analysis

Prism software (GraphPad Software Inc., San Diego, CA) was used to perform all statistical analyses. All results are expressed as means ± SEMs. The significance of differences between two sample means was determined by unpaired, two-tailed Student *t* tests, using 95% confidence intervals. A *P* value of less than 0.05 was considered significant.

RESULTS

Efnb2 Is Distributed in SPC-Expressing Epithelial Cells in Embryonic and Adult Lungs

To determine the role of ephrin-B2 in pulmonary development, we used an *Efnb2* knock-in mutant mouse that expresses a truncated protein in which the cytoplasmic domain is replaced by β-galactosidase to eliminate reverse signaling, while retaining the ability to bind and interact with its EphB receptors to initiate forward signaling. $EfnB2^{LacZ/+}$ heterozygote mice are viable, and permitted the analysis of ephrin-B2 protein distribution throughout pulmonary development into adulthood, because a reduced amount of reverse signaling is preserved. In contrast, $EfnB2^{LacZ/LacZ}$ homozygous mice are neonatal lethal, with cardiac and other midline defects (8, 14). The X-gal staining of whole-mount embryonic (E) Day 11.5 lungs revealed a diffuse distal airway distribution, as evidenced by the staining of airway branches (Figures 1A and 1B). An analysis of OCT sections on Days E11.5, E13.5, and E15.5 revealed a staining distribution consistent with epithelial cells (Figures 1C–1H). Colocalization using SPC, an epithelial Type II cell marker in conjunction with X-gal, confirmed epithelial expression throughout pulmonary embryologic development (Figures 2A–2D). This persisted into adulthood, as shown by the LacZ distribution in collapsed (Figures 1I–1L) and inflation-fixed (Figures 1M–1P) lungs, and by the colocalization of SPC and LacZ (Figures 2E–2J; *see* also the low-magnification views in Figure E1 in the online supplement). In contrast to other proteins expressed in distal epithelial cells that influence lung-branching morphogenesis, the ablation of Efnb2 reverse signaling exerted no impact on distal lung branching in the embryonic lung (data not shown). Furthermore, no expression of Efnb2 was found in alveolar Type I cells (Figure E3). Lastly, although previous reports identified Efnb2 in pericytes and vascular smooth muscle cells (12, 22), we found no evidence for the colocalization of Efnb2 in smooth muscle cells (α–smooth muscle actin) in embryonic lungs (Figures 3A–3D) or adult lungs (Figures 3E–3G; *see also* low-magnification views in Figure E2).

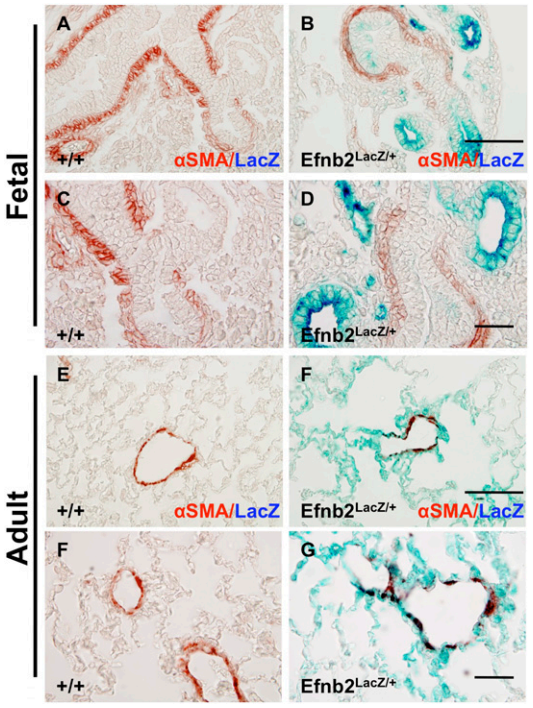

Figure 3. EfnB2 does not colocalize with α–smooth muscle actin (α-SMA) in the lung. Colocalization using β-gal and the smooth muscle marker α-SMA suggests that within the fetal lung (Day E13.5, *A–D*) or adult lung (age 8 wk, *E–G*), EfnB2 is not expressed in smooth muscle cells. Magnification in *A, B, E,* and *F, scale bar* = 50 μm; and in *C, D, F,* and *G, scale bar* = 20 μm.

Efnb2 Cytoplasmic Domain Mediates Distal Lung Dysplasia and Alveolar Crest Formation

The distal alveolar development of air-exchanging alveolar clefts and alveolar Type I cells actively continues postnatally. However, secondary to midline defects, ablation of the Efnb2 cytoplasmic domain is fatal at birth. To determine the role of Efnb2 reverse signaling in postnatal lung development, we used an $Efnb2^{LacZ/6YF\Delta V}$ transgenic mouse, in which the Efnb2 protein is correctly localized to the cell surface, but is unable to become tyrosine-phosphorylated or to interact with either SH2 or PDZ domain–containing downstream signaling proteins (18). Because Efnb2 expression was noted in the distal epithelium, adult mouse lungs were analyzed for structural and cellular differences. The disruption of Efnb2 reverse signaling significantly reduced air-exchanging distal alveolar crests (Figures 4B, 4D, and 4E). Furthermore, morphometric analysis determined that the distal alveoli were dysplastic, because the MLI was markedly elevated in $Efnb2^{LacZ/6YF\Delta V}$ mice (Figure 4F), compared with WT littermates (Figures 4A, 4C, 4E, and 4F). The analysis of epithelial cell types and numbers did not produce statistically significant results (Figures E4A–E4C). Because previous studies found an association between the PDZ domain and lymphatic development and Efnb2 (12, 13), lung weight and pulmonary lymphatic vessel density were examined. The alteration of reverse signaling with either the SH2 or PDZ domain exerted no impact on pulmonary lymphatic formation (Figure E4D), ratios of lung dry/wet weight (Figure E4E), or myocardial weight (Figure E4F) (minimum of six animals per group, Student *t* test).

Efnb2 Reverse Signaling Significantly Affects Pulmonary Function

Structural pulmonary irregularities are frequently associated with abnormal lung function. Pulmonary function testing was

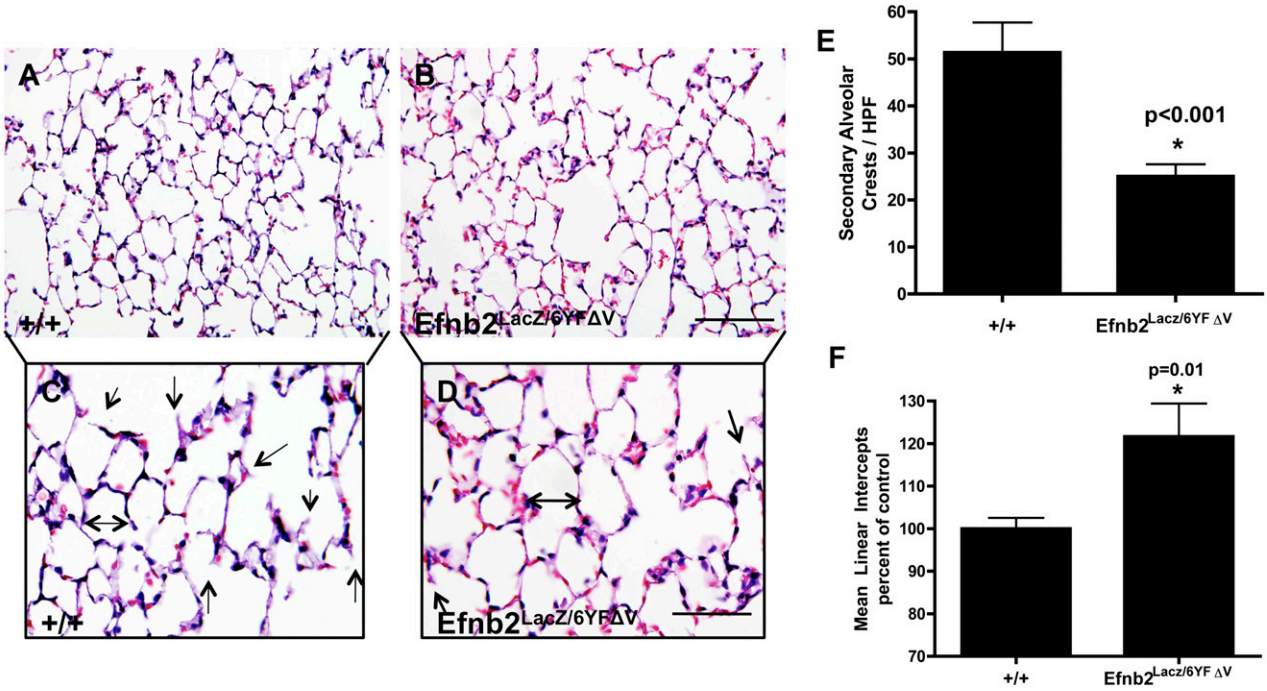

Figure 4. Alterations of EfnB2 reverse signaling disrupted distal lung morphometry. Hematoxylin-and-eosin–stained sections from EfnB2$^{LacZ/6YF\Delta V}$ adult inflation-fixed lungs (at age 8 wk) indicated that alterations of reverse Efnb2 signaling exhibited a significant ($P < 0.001$) reduction in secondary alveolar crests at age 8 weeks (*B* and *D*, *arrows* identify alveolar crests) compared with wild-type control mice (*A* and *C*, *arrows* identify alveolar crests; see also *E*). Furthermore, the mean linear intercept was significantly ($P = 0.01$) increased at age 8 weeks in EfnB2$^{LacZ/6YF\Delta V}$ mice (*B* and *D*, *double-headed arrow*; see also *F*), consistent with alveolar hypoplasia, compared with WT control mice (*A* and *C*, *double-headed arrow*; see also *F*). An *asterisk* denotes that statistical significance was reached. Magnification in *A* and *B*, *scale bar* = 50 μm; and in *C* and *D*, *scale bar* = 25 μm.

performed to determine the impact that the disruption of Efnb2 reverse signaling exerted on lung mechanics. Efnb2$^{LacZ/6YF\Delta V}$ mice demonstrated a significant increase in lung-tissue elastance (H in Figure 5B) and tissue damping (G in Figure 5C) ($n = 6$/group, $P = 0.04$ and $P = 0.0185$, respectively, according to unpaired Student *t* test), whereas airway resistance was reduced, but not to a statistically significant extent (RN in Figure 5A), and hysteresivity was unchanged (Figure 5D) compared with WT control mice. Next, conventional P–V measurements were performed on degassed lungs to determine quasistatic lung compliance. The mean P–V curves were plotted, and the specific lung compliance was calculated. The P–V curve derived from Efnb2$^{LacZ/6YF\Delta V}$ mice demonstrated a marked shift downward and to the right, and revealed a reduction in hysteresis in comparison with the P–V curve generated from WT mice (Figure 5E). Consistent with this observation, the calculated specific lung compliance was significantly decreased in ephrin–Efnb2$^{LacZ/6YF\Delta V}$ mice (Figure 5F; $n = 4$–5/group; $P = 0.02$, according to unpaired Student *t* test).

Altered Efnb2 Reverse Signaling Markedly Increases Pulmonary FN Deposition and Associated α5 Integrin Expression

Because decreased pulmonary compliance has been associated with changes in the extracellular matrix (ECM), because equal amounts of SPC were expressed in Efnb2$^{LacZ/6YF\Delta V}$ and WT control mice, and because recent zebrafish studies showed a direct link between Efnb2 reverse signaling and FN matrix assembly at the somite borders (23, 24), we explored FN matrix assembly in the lungs of Efnb2$^{LacZ/6YF\Delta V}$ mice. Alterations in Efnb2 reverse signaling markedly increased insoluble FN basement-membrane matrix assembly, as shown by both immunofluorescence (Figures 6B and 6D; *arrows* indicate FN fibrillogenesis) and Western blot analysis (Figure 6F, $n = 4$/group, normalized to equal protein loading and soluble FN; $P = 0.0034$, according to unpaired Student *t* test), compared with WT littermates (Figures 6A and 6C). Furthermore, an associated significant increase was evident in the α5 integrin required for FN fibrillogenesis (Figure 6G, $n = 4$/group; $P = 0.01$, according to unpaired Student *t* test).

DISCUSSION

Although angiogenesis is widely described as influencing pulmonary morphogenesis, the molecular events during vessel formation that drive alveolarization have not been determined. One such vascular mediator is the tyrosine kinase ligand ephrin-B2. Expressed in primitive arterial vessels, the EfnB2 ligand is an essential protein whose ablation is uniformly fatal in the embryonic stage of development because of failed angiogenic remodeling. Using a mouse knock-in model in which the intracellular domain of ephrin-B2 was replaced by bacterial β-gal sequences, we determined that this protein is expressed in alveolar Type II (AT2) cells throughout embryonic lung development and into adulthood. Furthermore, deletions and point mutations of key residues within the ephrin-B2 intracellular domain established that reverse signaling is critical for normal distal alveolarization. In conjunction with the alterations in distal airway morphometry, a marked disruption in distal lung mechanics was evident, with a reduction in lung compliance and a marked increase in distal lung FN fibrillogenesis and matrix deposition. These findings indicate that the vascular mediator ephrin-B2 plays an integral role in the structural formation of functional gas-exchanging alveoli that reaches beyond the limitations of the endothelium.

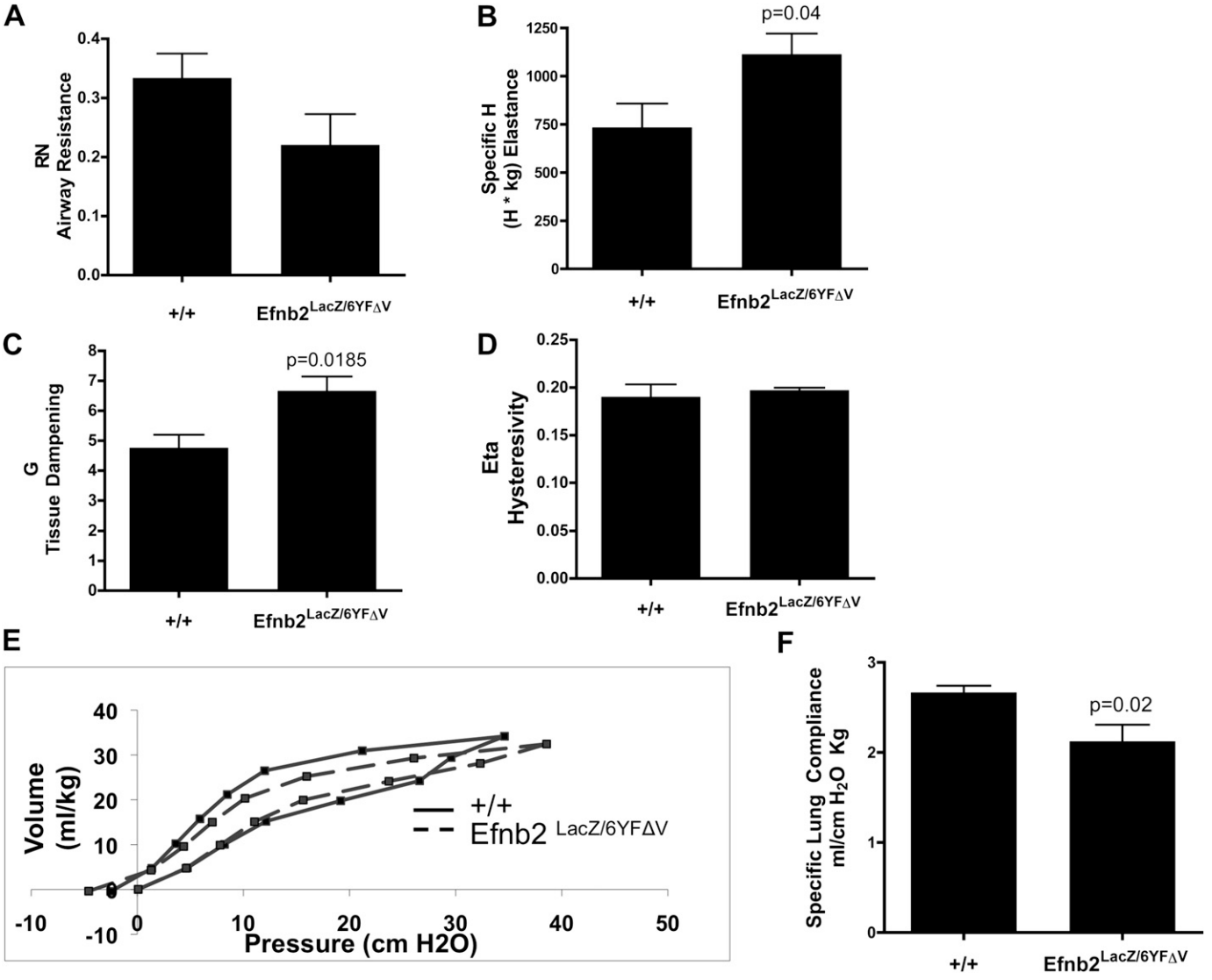

Figure 5. Altered EfnB2 reverse signaling significantly affects lung mechanics. Pulmonary function tests determined that 8-week-old mice with disrupted reverse Efnb2 signaling exhibited a significant increase in elastance (*B*, $P = 0.04$) and tissue damping (*C*, $P = 0.0185$). Consistent with these findings, a marked decrease in lung compliance (*F*, $P = 0.02$) was evident, with a shift down and to the right, and diminished hysteresis of the volume–pressure loops (*E*, *dotted lines*) in Efnb2$^{LacZ/6YF\Delta V}$ mice compared with WT littermates (*E*, *solid lines*), consistent with lungs that demonstrate increased resistance. Airway resistance (*A*), tissue damping (*C*), and hysteresivity (*D*) were similar between the groups.

A precise balance of angiogenic and antiangiogenic mediators throughout pulmonary development is pivotal in the formation of distal alveoli with gas-exchanging properties (1). The targeted pulmonary genetic manipulation of vascular mediators (25–27) and the delivery of exogenous vascular inhibitors (4, 28, 29) during lung development profoundly disrupt vessel formation and strikingly inhibit alveolar growth. Because of the intricate connection between vascularization and lung branching, it is not surprising that lung development is vulnerable to vascular manipulation and can result in disruption of the alveolar–capillary interface. Ephrin-B2 is involved in angiogenesis, and is defined as a marker of endothelial arterial fate specification. However, in contrast to other vascular markers such as platelet endothelial cell adhesion molecule–1 or vascular endothelial cadherin, we identified a distinct and extensive epithelial distribution of ephrin-B2 in the distal airways that extends beyond the confines of the pulmonary developmental period. This prolonged coexpression of a vascular marker in alveolar cells suggests that ephrin-B2 plays a greater role in lung development than just the formation of capillaries and blood vessels. Although previous studies identified an association between the ephrin-B2 cytoplasmic domain, alterations in lung morphometry, altered fibrillin distribution, and some weakly positive SPC cells colocalizing with ephrin-B2 (16), our study is the first to establish that this molecule is expressed throughout development and into adulthood in AT2 cells. Furthermore, the distribution and expression pattern of ephrin-B2 in the developing lung may potentially mark early progenitor cells that are destined for distal structures, and may serve as a useful marker for presumptive Type II cells. However, in contrast to other epithelial developmentally expressed proteins, the alteration or ablation of ephrin-B2 reverse signaling exerted no impact on branching (data not shown). A recent study by Vadivel and colleagues (17) identified a critical role for ephrin-B2 in lung growth and repair, when they demonstrated that the transient short, interfering RNA knockdown *in vivo* of ephrin-B2 in

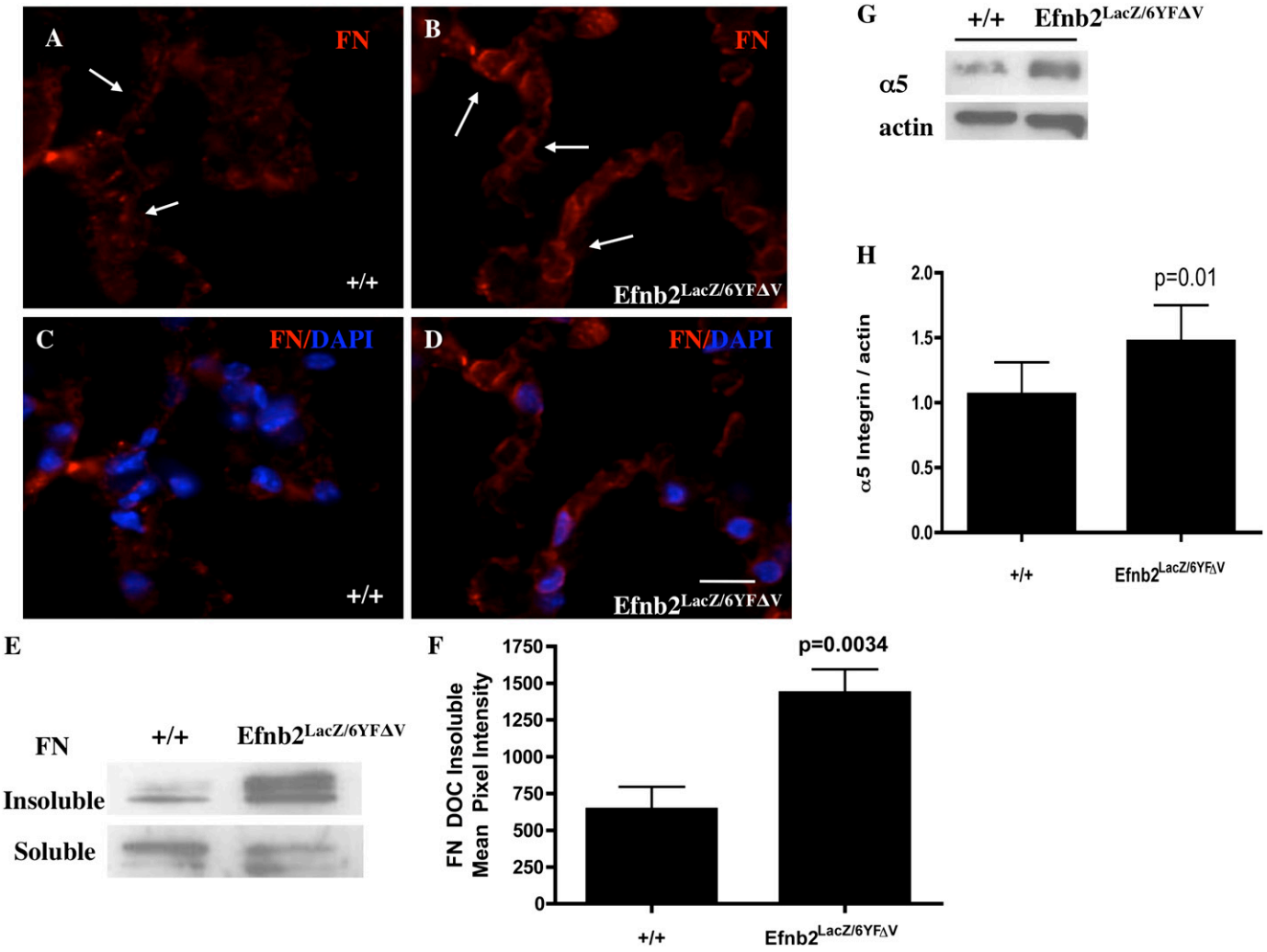

Figure 6. Ephrin-B2 reverse signaling mediates distal lung fibrillar fibronectin (FN) deposition. Insoluble fibrillar FN expression was markedly increased in immunofluorescent analyses of distal alveoli cell–cell junctions (in *B* and *D*, *arrows* identify the insoluble fibrillar FN that is laid down as strands of FN; Cy3 was the secondary antibody, and 4′6-diamidino-2-phenylindole [DAPI] denotes a nucleus) and immunoblotting (*E* and *F*, equal protein loading, and soluble Fn serves as loading control) in 8-week-old Efnb2$^{LacZ/6YF\Delta V}$ mice compared with WT mice (*A*, *arrows* demonstrate minimal fibrillar FN; *C*, immunofluorescence; *E* and *F*, Western Blot analysis). In addition, α5 integrin expression was markedly increased (*G* and *H*, $P = 0.01$) in Efnb2$^{LacZ/6YF\Delta V}$ mice, compared with WT control mice (*G* and *H*). Magnification in *A–D*, *scale bar* = 20 μm.

newborn rats induced a severe alveolar simplification, similar to the alveolar simplification found in the genetically manipulated mice in our experiments. Although previous studies targeted the reverse and forward signaling of ephrin-B2, our study focused only on the reverse signaling component. Dissecting how ephrin-B2 reverse signaling may affect lung regeneration after injury remains the primary focus of our ongoing work.

Distinct from other studies of vascular mediators in lung development, we identified a direct connection between this vascular mediator and abnormal pulmonary mechanics. Alterations of the reverse signaling process significantly decreased lung compliance, while increasing elastance and tissue damping. In conjunction with altered distal lung morphometry, these findings are most consistent with the clinical lung disease emphysema. Mechanistically, little is known regarding the role of ephrin-B2 reverse signaling in pulmonary development. However, the analysis of SPC levels eliminated the effects of surfactant on compliance. Recently, zebrafish studies showed a direct link between ephrin-B2 reverse signaling and ECM formation. The engagement of ephrin-B2 with an Eph receptor initiated epithelial cell surface clustering of the α5β1 integrin in the zebrafish somite, resulting in the binding of soluble FN, intracellular signaling, and subsequent FN matrix assembly (23, 24). FN, a multifunctional adhesive glycoprotein, is a prolific ECM protein that is essential for normal development (30). Secreted as a disulfide-bonded dimer, it binds principally to cell surface integrins. The binding of FN to integrins results in the unfolding of this soluble protein, and its further assembly results in a detergent-insoluble fibrillar matrix (i.e., fibrillogenesis). Although ephrin-B2 ablation in the somites eliminated FN deposition at the somite borders (23, 24, 31), our experiments identified a marked increase in FN fibrillogenesis in the distal alveolar regions of *Efnb2*$^{LacZ/6YF\Delta V}$ mice. These findings support a role for ephrin-B2 reverse signaling in the damping of FN fibrillogenesis.

In conclusion, our experiments show for the first time a functional role for ephrin-B2 reverse signaling in the pulmonary epithelium and its impact on lung morphometry and mechanics. Furthermore, our findings suggest a role for reverse signaling in the suppression of pulmonary FN fibrillogenesis. These

findings broaden our current understanding of the role played by ephrin-B2 in pulmonary development, a role that extends beyond arterial endothelial guidance.

Author disclosures are available with the text of this article at www.atsjournals.org.

Acknowledgments: The authors thank Olatunji Williams for his technical support.

References

1. Schwarz M, Cleaver O. Development of the pulmonary endothelium in development of the pulmonary circulation: vasculogenesis and angiogenesis. In: Voelkel NF, Rounds S, editors. The pulmonary endothelium. Chichester, United Kingdom: John Wiley and Sons, Ltd.; 2009. pp. 3–24.
2. Chen Y, Legan SK, Mahan A, Thornton J, Xu H, Schwarz MA. Endothelial monocyte activating polypeptide II disrupts alveolar epithelial Type II to Type I cell transdifferentiation. *Respir Res* 2012;13:1.
3. Schwarz MA, Wan Z, Liu J, Lee MK. Epithelial–mesenchymal interactions are linked to neovascularization. *Am J Respir Cell Mol Biol* 2004;30:784–792.
4. Schwarz MA, Zhang F, Gebb S, Starnes V, Warburton D. EMAP II inhibits lung neovascularization and airway epithelial morphogenesis. *Mech Dev* 2000;95:123–132.
5. Schwarz MA, Zheng H, Legan S, Foty RA. Lung self-assembly is modulated by tissue surface tensions. *Am J Respir Cell Mol Biol* 2011; 44:682–691.
6. Davy A, Soriano P. Ephrin signaling *in vivo*: look both ways. *Dev Dyn* 2005;232:1–10.
7. Cowan CA, Henkemeyer M. The SH2/SH3 adaptor GRB4 transduces B-ephrin reverse signals. *Nature* 2001;413:174–179.
8. Cowan CA, Yokoyama N, Saxena A, Chumley MJ, Silvany RE, Baker LA, Srivastava D, Henkemeyer M. Ephrin-B2 reverse signaling is required for axon pathfinding and cardiac valve formation but not early vascular development. *Dev Biol* 2004;271:263–271.
9. Adams RH, Wilkinson GA, Weiss C, Diella F, Gale NW, Deutsch U, Risau W, Klein R. Roles of ephrinB ligands and EphB receptors in cardiovascular development: demarcation of arterial/venous domains, vascular morphogenesis, and sprouting angiogenesis. *Genes Dev* 1999; 13:295–306.
10. Wang HU, Chen ZF, Anderson DJ. Molecular distinction and angiogenic interaction between embryonic arteries and veins revealed by ephrin-B2 and its receptor Eph-B4. *Cell* 1998;93:741–753.
11. O'Leary DD, Wilkinson DG. Eph receptors and ephrins in neural development. *Curr Opin Neurobiol* 1999;9:65–73.
12. Foo SS, Turner CJ, Adams S, Compagni A, Aubyn D, Kogata N, Lindblom P, Shani M, Zicha D, Adams RH. Ephrin-B2 controls cell motility and adhesion during blood-vessel–wall assembly. *Cell* 2006;124:161–173.
13. Makinen T, Adams RH, Bailey J, Lu Q, Ziemiecki A, Alitalo K, Klein R, Wilkinson GA. PDZ interaction site in ephrinB2 is required for the remodeling of lymphatic vasculature. *Genes Dev* 2005;19:397–410.
14. Dravis C, Yokoyama N, Chumley MJ, Cowan CA, Silvany RE, Shay J, Baker LA, Henkemeyer M. Bidirectional signaling mediated by ephrin-B2 and EphB2 controls urorectal development. *Dev Biol* 2004; 271:272–290.
15. Schwarz MA, Caldwell L, Cafasso D, Zheng H. Emerging pulmonary vasculature lacks fate specification. *Am J Physiol Lung Cell Mol Physiol* 2009;296:L71–L81.
16. Wilkinson GA, Schittny JC, Reinhardt DP, Klein R. Role for ephrinB2 in postnatal lung alveolar development and elastic matrix integrity. *Dev Dyn* 2008;237:2220–2234.
17. Vadivel A, van Haaften T, Alphonse RS, Rey-Parra GJ, Ionescu L, Haromy A, Eaton F, Michelakis E, Thebaud B. Critical role of the axonal guidance cue ephrinB2 in lung growth, angiogenesis, and repair. *Am J Respir Crit Care Med* 2012;185:564–574.
18. Thakar S, Chenaux G, Henkemeyer M. Critical roles for EphB and ephrin-B bidirectional signalling in retinocollicular mapping. *Nat Commun* 2011;2:431.
19. Dravis C, Henkemeyer M. Ephrin-B reverse signaling controls septation events at the embryonic midline through separate tyrosine phosphorylation–independent signaling avenues. *Dev Biol* 2011;355:138–151.
20. Robinson EE, Foty RA, Corbett SA. Fibronectin matrix assembly regulates alpha5beta1-mediated cell cohesion. *Mol Biol Cell* 2004; 15:973–981.
21. Weibel E. Stereological methods volume 1: practical methods for biological morphometry. London: Academic Press; 1979.
22. Gale NW, Baluk P, Pan L, Kwan M, Holash J, DeChiara TM, McDonald DM, Yancopoulos GD. Ephrin-B2 selectively marks arterial vessels and neovascularization sites in the adult, with expression in both endothelial and smooth-muscle cells. *Dev Biol* 2001;230:151–160.
23. Julich D, Mould AP, Koper E, Holley SA. Control of extracellular matrix assembly along tissue boundaries via integrin and Eph/ephrin signaling. *Development* 2009;136:2913–2921.
24. Koshida S, Kishimoto Y, Ustumi H, Shimizu T, Furutani-Seiki M, Kondoh H, Takada S. Integrinalpha5-dependent fibronectin accumulation for maintenance of somite boundaries in zebrafish embryos. *Dev Cell* 2005;8:587–598.
25. Zeng X, Wert SE, Federici R, Peters KG, Whitsett JA. VEGF enhances pulmonary vasculogenesis and disrupts lung morphogenesis *in vivo*. *Dev Dyn* 1998;211:215–227.
26. Galambos C, Ng YS, Ali A, Noguchi A, Lovejoy S, D'Amore PA, DeMello DE. Defective pulmonary development in the absence of heparin-binding vascular endothelial growth factor isoforms. *Am J Respir Cell Mol Biol* 2002;27:194–203.
27. Ruhrberg C, Gerhardt H, Golding M, Watson R, Ioannidou S, Fujisawa H, Betsholtz C, Shima DT. Spatially restricted patterning cues provided by heparin-binding VEGF: a control blood vessel branching morphogenesis. *Genes Dev* 2002;16:2684–2698.
28. Jakkula M, Le Cras TD, Gebb S, Hirth KP, Tuder RM, Voelkel NF, Abman SH. Inhibition of angiogenesis decreases alveolarization in the developing rat lung. *Am J Physiol Lung Cell Mol Physiol* 2000;279:L600–L607.
29. DeLisser HM, Helmke BP, Cao G, Egan PM, Taichman D, Fehrenbach M, Zaman A, Cui Z, Mohan GS, Baldwin HS, *et al.* Loss of PECAM-1 function impairs alveolarization. *J Biol Chem* 2006;281:8724–8731.
30. Hynes RO. Fibronectins. New York: Springer-Verlag; 1990.
31. Larsen M, Artym VV, Green JA, Yamada KM. The matrix reorganized: extracellular matrix remodeling and integrin signaling. *Curr Opin Cell Biol* 2006;18:463–471.